MedCrave
Step into the World of Research
Journal of Nutritional Health & Food Engineering

Research Article
Open Access
CrossMark

Biodegradable films composed of active nanopolyphenolic compounds extracted from olive leaves and pomace for food packaging applications

Abstract

This study aimed to develop biodegradable, active, edible films based on calcium alginate, incorporating nanopolyphenolic antimicrobials from olive leaf extract (OLE) and olive pomace extract (OPE), combined with ZnO nanoparticles (ZnONPs) in a nanoemulsion. The nanoemulsion and film-forming solutions were characterized by particle size distribution, zeta potential, rheology, FTIR, and scanning electron microscopy (SEM). Film properties (thickness, tensile strength, elongation, and solubility) were evaluated, and the resulting coatings/films were applied to fresh persimmon fruit stored at 5 ± 1°C and 90–95% RH for 20 days. Compared with the uncoated control (A), all nano-coated treatments (B–D) reduced microbial growth, slowed physicochemical deterioration, and extended shelf life, with antimicrobial effectiveness increasing with higher nanoemulsion concentration (B < C < D). The improved preservation performance was attributed to the combined action of phenolic compounds and ZnONPs, which enhanced film stability and functionality while maintaining acceptable sensory quality and suitable gas and moisture barrier properties. Overall, calcium alginate films enriched with OLE/OPE–ZnONPs nanoemulsions show promise as potentially effective, low-cost edible coatings/films for fruit preservation and broader food packaging applications

Keywords: fresh persimmons fruit, shelf-life, biodegradable films, calcium alginate, action of phenolic compounds in Olive Leaves Extract (OLE) and Olive pomace Extract (OPE)/ZnONPs synthetic nanoemulsion

Volume 14 Issue 2 - 2026

Hosam El Din Aboul anean,[1] Mohamed Abdin,[1] Eman A Abdel Khafar,[1] Munirah Fayez Almudarra,[2] L O Mallasiy[3]

[1]Food Engineering and Packaging Department, Food Technology Research Institute (FTRI), Agriculture Research Center (ARC), Egypt
[2]College of Education Prince Sattam bin Abdulaziz University, Saudi Arabia
[3]Department of Health Sciences, Basic Sciences, and Their Applications, Muhayil Asir, Applied College, King Khalid University, Saudi Arabia

Correspondence: Hosam el din Aboul anean, Food Technology Research Institute, Agricultural Research Center, Egypt, Tel +20-011 1266 7765, +20-010 1884 2643

Received: May 18, 2026 | **Published:** July 07, 2026

Introduction

Active packaging is an innovative food packaging technology designed to extend the shelf life and maintain the quality and safety of food products. Unlike conventional packaging, which acts mainly as a passive barrier, active packaging interacts with the food or its surrounding environment to improve preservation. It can release or absorb substances such as antioxidants, antimicrobial agents, oxygen, moisture, or ethylene to slow food deterioration. Natural bioactive compounds, particularly polyphenols from agricultural by-products like olive leaves and olive pomace, are increasingly used as active agents due to their antioxidant and antimicrobial properties. Incorporating these compounds into biodegradable polymer films creates environmentally friendly packaging materials with enhanced functionality. Such active biodegradable films help reduce food waste, improve food safety, and decrease dependence on petroleum-based plastics, supporting sustainable food packaging solutions.[1] In recent years, increasing attention has been directed toward the development and expansion of smart and active biodegradable packaging. These advanced packaging systems aim to improve food preservation strategies and maintain product integrity through the incorporation of biologically active compounds. Active packaging in particular, has become increasingly important in preserving food products and is gaining widespread popularity in global markets. It is considered a new type of packaging capable of responding to changes in the packaged product during storage. This is achieved through the integration of sensors or indicators that are attractive, easy to use, and cost-effective, thereby enhancing consumer confidence. Such systems are designed to ensure safer food, extend shelf life, and enable real-time monitoring of food quality. These functions can be further enhanced by incorporating nanomaterials and nanocomposites, which can provide information about food safety and consumption status. Smart packaging operates through internal or external systems, such as sensors or indicators, that provide data on storage history and product quality. Olive tree cultivation, virgin olive oil production, and olive pomace extraction generate significant amounts of waste and by-products, including leaves, wood, olive pomace, and exhausted or defatted pomace. These wastes are often difficult to manage and can lead to environmental problems. Therefore, developing alternative uses for these bioresources to produce high value-added products has become a research priority. Recent studies have explored the utilization of olive residues and by-products—such as olive leaves, pruning's, pomace, and exhausted pomace—for the extraction of valuable compounds.[2] Olive pomace, the solid residue remaining after olive oil extraction, is one of the most abundant agro-industrial by-products in the Mediterranean region and poses environmental challenges due to its accumulation and disposal.[3,4] In Egypt, approximately 60 million olive trees generate large quantities of pomace and leaf waste.[5] Typically, 100 kg of olives produce about 35 kg of raw pomace. Although pomace can be used as feed for ruminants, its high content of cell wall components makes it unpalatable and poorly digestible. Various chemical treatments have been attempted to improve its nutritional value, with limited success.[6] Olive oil extraction generally yields pomace and oil in an approximate ratio of 80:20, depending on the extraction method and olive variety.[7] With the expansion of olive cultivation in Egypt, concerns about environmental issues arising from improper waste disposal have increased. Pomace is often used as a soil fertilizer.[8] Nutritionally, pomace contains lipids (11.5%), proteins (8.9%), ash (4%), and dietary fiber (54.5%) per 100 g.[9] It is also rich in phenolic compounds, reaching up to 34.04 mg gallic acid equivalents per gram of plant material. The main phenolic compounds include hydroxytyrosol, oleuropein, vanillin, apigenin, rutin, and luteolin.[10,11] These beneficial nutritional and functional properties make olive pomace an attractive ingredient for food applications,

particularly in bakery products. The incorporation of olive leaf extract (OLE) into polymer films for food packaging applications has gained increasing interest. Advances in food packaging play a crucial role in maintaining food freshness, safety, and environmental sustainability.[12] Consumers increasingly demand food that is fresh, high-quality, safe, and environmentally friendly, with a growing emphasis on reducing waste and using biodegradable packaging materials. Food packaging materials are essential for ensuring food safety, preserving quality, and extending shelf life by preventing deterioration caused by microbial spoilage, oxidation, and metabolic processes. Packaging also protects food from environmental factors such as light, temperature, humidity, physical damage, dust, odors, and microorganisms. Epidemiological studies indicate a significant increase in foodborne illnesses caused by various pathogens.[13] Therefore, controlling microbial growth is critical for improving food safety. Natural bioactive compounds derived from plants, herbs, and essential oils exhibit antimicrobial and antioxidant properties and can be incorporated into packaging materials to inhibit foodborne microorganisms and extend shelf life.[14] Active packaging is an emerging field in which antimicrobial agents are embedded within packaging materials to interact with food and control microbial growth. This approach is considered a promising strategy for enhancing food safety.[15–18] Antimicrobial food packaging represents one of the most innovative aspects of active packaging, as it can reduce, inhibit, or delay microbial growth on food surfaces or within packaging materials, thereby extending shelf life.[19] Consequently, researchers are increasingly exploring plant extracts and natural compounds to modify polymer materials and impart antibacterial and antioxidant properties. Olive leaf extract has been widely used to enhance various polymer-based films, including chitosan (CTS), carrageenan (CN), polyvinyl alcohol/cellulose nanofibers, and cellulose nanocrystals/poly(butylene adipate-co-terephthalate) films.[20,21] Films enriched with OLE typically exhibit strong antioxidant activity due to their high polyphenol content. CTS/OLE films, for example, demonstrate reduced water vapor permeability, improved solubility in food simulants, and antimicrobial activity against pathogens such as *L. monocytogenes* and *C. jejuni*. These properties have been confirmed through in situ studies on chicken products. Although OLE exhibits inhibitory effects on bacterial growth, it is not fully bactericidal at higher temperatures.[22]

Additionally, incorporating OLE into chitosan films enhances mechanical properties such as tensile strength, elongation, and moisture retention capacity.[23] Whereas, adding too much or too little ZnO can ruin the film. Researchers look for an optimal threshold where antimicrobial activity is high, but Zn2+ migration stays below the 5 mg/kg safety ceiling. The Minimal Effective Dose (1% w/w): Even at low loadings of 1% zinc oxide by weight of total solids, films begin to exhibit noticeable UV-blocking properties and moderate antimicrobial activity against pathogens like E. coli and S. aureus.[24] The Optimal Sweet Spot (3% w/w): Across multiple biopolymer solutions (such as gelatin, starch, and pectin), 3% ZnO is widely considered the mechanical and physical optimum.[25] At 3%, the film maximizes tensile strength and oxygen/UV barrier properties without becoming overly brittle. The Upper Limit Threshold (5% w/w): While 5% blends provide the strongest antimicrobial clear zones, concentrations at or above this mark often trigger significant agglomeration (clumping) of particles.[25] This clumping creates structural micro-cracks, increases water vapor permeability, reduces elasticity, and accelerates unpredictable ion leaching. Factors Influencing Safe Application. If you are developing a food film solution, keep these variables in mind to stay within permissible migration levels: Food Matrix pH (Crucial Risk Factor)

The stability of ZnO is highly pH-dependent. At a neutral pH, less than 5% of Zn^{2}+ ions are released from the film. However, if the film comes into contact with acidic foods (pH less than 3.5), the dissolution rate spikes dramatically, releasing up to 88% of the bound zinc within 48 hours.[26] This can easily cause the food to exceed the 5 mg/kg SML. Nanoparticle vs. Bulk Form: Nanoparticles (≤ 100 nm) offer superior antimicrobial surface area but migrate differently than bulk zinc. Regulatory bodies mandate that nanoparticles must be securely immobilized within the polymer matrix so that only the safe, ionic Zn2+ transfers to the food surface, rather than the intact nanoparticles themselves.[26] The objective of this study was to develop edible nanofilms based on calcium alginate incorporated with nanoemulsions of polyphenolic compounds derived from olive leaves (NCPCOLE) and olive pomace extract (NCPCOPE). These nanoemulsions were used to produce edible coatings and films loaded onto calcium alginate matrices. The physical and mechanical properties of the films—including viscosity, water vapor permeability, particle size distribution, zeta potential, color, light transmittance, and microstructure (SEM)—were evaluated. The study also aimed to determine the effectiveness of these coatings in improving the storability of fresh persimmon fruit during cold storage, as well as in reducing microbial growth and physicochemical deterioration during storage.

Materials and methods

Olive leaf extract (OLE)

Olive leaves and pomace (Maraqi variety), which are widely cultivated in the Siwa Oasis, were obtained during the winter season of 2023/2024 from the Agricultural Research Center, Giza, Egypt. The samples were cleaned to remove impurities and foreign materials, then stored in a dry place at room temperature (25 ± 2 °C) for subsequent extraction.

All experimental work was conducted at the Central Laboratory of Agricultural Research, Food Engineering and Packaging Department, Food Technology Research Institute, Agricultural Research Center, Giza, Egypt, to prepare phenolic compounds from olive leaf extract (OLE) and olive pomace extract (OPE) nanoparticles for the production of nano-bio-composite films.

The materials used included 95% ethyl alcohol, chloroform, and methanol (El-Nasr Pharmaceutical Chemicals Company, Cairo, Egypt). Sulfuric acid (H2SO4) and hydrochloric acid (HCl) were obtained from El-Gomhouria Chemical Company. Glycerol and sodium hydroxide were supplied by Acmatic for Chemicals & Lab Equipment Company, Cairo, Egypt. Glacial acetic acid was obtained from Across Organics, Belgium. Whatman No. 1 filter paper and a 50-mesh sieve were obtained from Across Organics, New Jersey, USA. Glutaraldehyde was purchased from Win Lab Company (UK), and Tween 80 was obtained from Zhejiang Silver Elephant Bio-Engineering Co., Ltd., China. Sodium chloride (NaCl) was obtained from Jenapharm.

Preparation of olive leaf extract (OLE)

A 20 g portion of dried and finely ground olive leaf powder (80 mesh) was extracted using ethanol (ethanol: Water, 80:20 v/v) and aqueous ethyl acetate (ethyl acetate: Water, 80:20 v/v) (200 mL) for 6 h at room temperature using an orbital shaker in a water bath. The extracts were separated from the residues by filtration through Whatman No. 1 filter paper to remove coarse particles.

The combined filtrates were concentrated and the solvent was removed under reduced pressure at 45°C using a rotary evaporator

under vacuum. Maceration was then carried out for 1 h at ambient temperature in a dark environment. The concentrated extracts were stored at 4°C until further use, following the methods of Alfonso M. Vidal et al., Saptarini, N. M., & Herawati, I. E., Nelson et al., and Grabska-Zielińska S.[23,27–29]

Preparation of olive pomace extract (OPE)

Five grams of olive pomace powder were suspended in 50 mL of an ethanol/water mixture (60:40, v/v) with stirring at 300 rpm. Extraction was performed at 50°C for 5 min using a sample-to-solvent ratio of 1:10 (g/mL). The extract was then separated by filtration using Whatman No. 1 filter paper.

The filtered extracts were concentrated and freed of solvent under reduced pressure at 45°C using a rotary evaporator under vacuum. Maceration was conducted for 1 h at ambient temperature in a dark place. The concentrated extracts were stored at 4°C until use.[30]

Preparation of nanoemulsion polyphenolic compounds (OLE/OPE) with ZnONPs

Ten milliliters of each phenolic extract (OLE and OPE) were mixed with 5 mL of non-ionic surfactant Tween 80 (5% v/v; 30% w/w of OLE/OPE) under gentle stirring until a homogeneous mixture was obtained. Distilled water (85 mL) was added to achieve a final volume of 100 mL, followed by magnetic stirring for 30 min.

The mixture was then sonicated for 30 min at 700 W using an ultrasonicator while maintained in an ice bath. The resulting extract was filtered through gauze and subsequently through Whatman No. 1 filter paper.

For ZnONPs synthesis, 0.5% (0.01% w/v) Zn precursor was added to the extract. After complete dissolution, 1 M KOH solution was added at a ratio of 1:6 (v/v) at room temperature. The synthesized nanoparticles were filtered and dried overnight in an oven at 70°C.[31]

Preparation of OLE/OPE nanoemulsion

Nanoemulsions of OLE and OPE were prepared with slight modifications. Tween 80 (HLB = 15) and distilled water were used as the surfactant and aqueous phase, respectively. The concentrations of OLE/OPE (5% v/v) and Tween 80 (30% w/w of OLE/OPE) were maintained constant.

A coarse emulsion was first prepared by gradually adding OLE/OPE and surfactant to water under continuous mixing at 3000 rpm. The coarse emulsion was then subjected to ultrasonic emulsification using a 20 kHz sonicator at 200 W. A sonotrode with a 15 mm probe was immersed to a depth of 25 mm, and sonication was carried out for 5 min. The temperature increase during the process was kept below 10°C.[32]

In another method, emulsions were prepared by mixing OLE/OPE (0.5% v/v) with Tween 20 (0.2% v/v) in Milli-Q water. The mixture was stirred for 20 min, followed by blending at 3000 rpm for 2 min and further mixing at 4000 rpm for 2 min. The coarse emulsions were then subjected to ultrasonication using a probe (13 mm diameter), with temperature controlled using an ice bath. Variables included amplitude (15–45 μm), treatment time (0.5–3 min), and surfactant type.[33]

Preparation of bionanocomposite edible films

The film-forming solution was prepared by slowly adding an aqueous lipid dispersion to a 2% calcium alginate solution at 70°C. Phenolic dispersions of OLE and OPE were prepared by homogenizing the extracts in 50 mL of deionized water at 70°C for 15 min.

Tween 80 (5% or 1.5%) and ZnONPs (0.5% or 0.01% w/v) nanoemulsion were added to ensure uniform distribution within the calcium alginate matrix. The mixture was homogenized at 4000 rpm for 15 min.

A plasticizer consisting of 50% glycerol and 50% polyethylene glycol (0.6 mL; 30% w/w of calcium alginate) was added to improve film flexibility. The solution was degassed using ultrasonication (400 Hz, 360 W) for 10–15 min at 25 ± 5°C. The resulting dispersion was cast onto Teflon-coated glass plates (20 × 20 cm) and dried at room temperature for approximately 72 h. The dried films were peeled off and stored at 25°C in the dark until further evaluation.

Experimental Design (Table 1),

Table 1 show up the formulas for nano edible film of prepared calcium alginate combined with nanoemulsionpolyphenolic compounds in Olive Leaves and pomace Extract to produce edible coating and films.

Film ingredient\nano ZnONPs & polyphenolic compounds					
Film code	**2% Calcium alginate**	**addition of plasticizer (50%glycerol+50%polyethyleneglycol) 0.6 ml at the level of 30%**	**5% (0.1 %) Tween 80 (30% wt) (w/v)of olive Leaves (OLE) extract nano emulsion**	**5% (0.1%) Tween 80 (30% wt) (w/v) of pomace extract nano emulsion (OPE)**	**Film cod ZnONPs 0.5%(0.01%)(w/v)**
A	2%	0.6	-	-	-
B	2%	0.6	5% (0.1%)	-	0.5%(0.01%)
C	2%	0.6	-	5% (0.1%)	0.5%(0.01%)
D	2%	0.6	5% (0.1%)	5% (0.1%)	0.5%(0.01%)

The edible nano-bio-composite films containing nanoemulsions of polyphenolic compounds were divided into four groups with different formulations to evaluate the effect of composition on film properties. The film-forming solution was modified accordingly and distributed into four equal parts for comparative evaluation.

- Treatment **A**: (Control): Film-forming solution based on calcium alginate nanoparticles only. A plasticizer consisting of 50% glycerol and 50% polyethylene glycol (0.6 mL; 30% w/w) was added.
- Treatment **B:** Calcium alginate nanoparticle-based films incorporated with 5% (0.1%) crude phenolic compounds derived from olive leaf extract (OLE) and 0.5% (0.01%) ZnONPs nanoemulsion.
- Treatment **C:** Calcium alginate nanoparticle-based films incorporated with 5% (0.1%) crude phenolic compounds derived from olive pomace extract (OPE) and 0.5% (0.01%) ZnONPs nanoemulsion.

- Treatment **D:** Calcium alginate nanoparticle-based films incorporated with 5% (0.15%) crude phenolic compounds derived from a combination of olive leaf extract (OLE) and olive pomace extract (OPE), along with 0.5% (0.01%) ZnONPs nanoemulsion.

Storage treatments of fresh persimmon fruits

Persimmon (*Diospyros kaki* L., "Fuyu" cultivar) fruits were obtained from a local farm in El-Kalubia Governorate, Egypt, grown in loamy soil under standard agricultural practices during the 2024 season. Fruits of uniform size, free from physical damage and fungal infection, were harvested at approximately three-quarters surface color maturity.

After harvest, fruits were packed in field boxes and transported to the laboratory, where they were stored overnight at 0.5°C. The following day, fruits were washed with tap water and disinfected by immersion in a calcium hypochlorite solution (0.25 g L^{-1}) for 2 min.

At the Central Laboratory of Agricultural Research and Food Technology Research Institute (Giza, Egypt), fruits were subjected to different coating treatments. Each group of fruits was dipped in the respective edible film solution for 1 min, then drained and packaged in plastic trays (approximately 500 g per tray).

All samples were stored at 5 ± 1°C and 90–95% relative humidity for 20 days in carton boxes. Storage experiments were conducted at the Postharvest Research Department, Horticulture Research Institute, Agricultural Research Center, Giza. Samples were periodically withdrawn during storage and analyzed for physical, chemical, microbiological, and properties until spoilage.

Physical, mechanical, and rheological properties of films

Rheological measurements: Rheological properties, including shear rate and shear stress, were measured to determine the optimal film-forming solutions. Measurements were conducted using a Brookfield DVN EXT viscometer (Brookfield Engineering Labs, AMETEK) at room temperature.

Samples were maintained at a constant temperature using a water bath. Measurements were performed at rotational speeds ranging from 10 to 60 rpm using spindle SC4-18. The flow behavior was described using the power-law model:

$$\tau = k\gamma^n$$

where:

τ = shear stress (Pa)

γ = shear rate (s^{-1})

k = consistency index coefficient($Pa \cdot s^n$)

n = flow behavior index [34]

Particle size and zeta potential: The particle size distribution and zeta potential of the nanoemulsions were measured using a Malvern Zetasizer Nano Series (Nano ZS, UK), with a size range of 0.6–6000 nm and zeta potential range of −200 to +200 mV.

Scanning electron microscopy (sem): The microstructure of calcium alginate films incorporated with OLE/OPE polyphenolic compounds and ZnONPs was examined using a high-resolution scanning electron microscope (Inspect S, FEI Company, Netherlands; Quanta FEG250). Samples were sputter-coated prior to analysis.[35]

Film thickness: Film thickness was measured using a digital micrometer (Mitutoyo Digital Indicator, Model PK-1012 E, Japan). Film strips were placed between the micrometer jaws, and the average of three readings was recorded for each sample.[36]

Color measurement: Color parameters (L*, a*, b*) were measured using a Minolta Chroma Meter (CR-200).The instrument was calibrated with a standard white plate before measurement.

- L* indicates lightness (0 = black, 100 = white)
- a* indicates red (+) to green (−)
- b* indicates yellow (+) to blue (−)

Color difference (ΔE*) was calculated using:

$$\ddot{A}E^* = \sqrt{\left(L^* - L_s^*\right)^2 + \left(a^* - a_s^*\right)^2 + \left(b^* - b_s^*\right)^2}$$

Where: L*, a* and b* represent the values of the film samples, L*s, a*s and b*s for the standard whiteboard **L*s** = 77.40, **a*s** = 1.44 and **b*s** = 8.62 values represented as background and take three readings for each film by Maria-Ioana Socaciu and Melinda Fogarasi[37] and ΔE = √ (L)2 + (a)2 + (b)2 where ΔL, a and b show the difference between each color value of the film sample and the standard plate respectively. According to Li., et al., and Munir et al.[38,39]

Light transmittance: Film transparency and barrier properties were evaluated by measuring light transmittance at wavelengths of 395, 430, and 550 nm using a LINSHANG LS108 transmission meter and a UV–VIS spectrophotometer (SPECTRUM VIS, China).

Film samples (0.7 × 3 cm) were placed in cuvettes, and absorbance was measured against a blank. Transmittance (%) was calculated from absorbance values. Transparent films typically exhibit transmittance values above 90%.[37,40,41]

Water solubility (%): The water solubility of calcium alginate nanoparticle films incorporated with 5% (0.15%) crude phenolic compounds from olive leaf extract (OLE) and olive pomace extract (OPE), along with 0.5% (0.01%) ZnONPs nanoemulsion, was determined for treatments A, B, C, and D.

Film samples were first dried in a desiccator containing calcium chloride. A known weight (500 mg) of each dried film sample was immersed in 50 mL of distilled water at room temperature for 24 h with gentle shaking. After immersion, the films were removed and re-dried in a desiccator to a constant weight.

Water solubility was calculated as percentage weight loss using the following equation:

$$\%\text{Weight loss} = \frac{\text{Initial dry weight} - \text{Final dry weight}}{\text{Initial dry weight}} \times 100$$ [34]

Mechanical properties: The mechanical properties (tensile strength and elongation at break) of calcium alginate nanoparticle films incorporated with OLE/OPE polyphenolic compounds and ZnONPs nanoemulsion were measured using a CT3 Texture Analyzer.

Film samples from treatments A, B, C, and D were cut into strips (3 × 5 cm). Each strip was fixed between the instrument jaws, and the jaws were moved at a constant speed until the film ruptured. Tensile strength and elongation were automatically recorded.[42]

Water vapor permeability (WVP): Water vapor transmission rate (WVTR) and water vapor permeability (WVP) were determined according to the ASTM E96-95 method.

Circular film samples were placed over test cups containing distilled water and sealed with paraffin oil. The cups were then placed in a desiccator containing calcium chloride. The weight of each cup was recorded hourly over a period of 10 h.

WVTR was calculated as:

$$WVTR = \frac{\Delta m}{\Delta t \times A}$$

WVP was calculated as:

$$WVP = \frac{WVTR \times L}{\Delta RH}$$

where:

$\Delta m / \Delta t$ = moisture gain per unit time (g/s)

A = film surface area (m²)

L= film thickness (mm)

ΔRH = relative humidity difference (ASTM E96-95)

Gas permeability: Gas permeability (O_2 and CO_2) was measured at 30°C using a stainless-steel cell and a Witt Oxybaby Headspace Gas Analyzer (O_2/CO_2 Gas Tester Model), following the method of Zahedia Y, et al. and García et al.[43,44]

Gas permeability (P) was calculated using the following equation:

$$P = \frac{Q \times X}{A \times t \times \Delta p}$$

Where:

P = gas permeability (m³/m·day·mmHg)

Q = volume of gas diffused (m³)

X = film thickness (mm)

A = film area (m²)

t = time (day)

Δp = pressure difference across the film at different treatments A, B, C and D.

FTIR analysis: Fourier Transform Infrared (FTIR) spectra were recorded using a Bruker Invenio S (USA) equipped with a Platinum Diamond ATR accessory. Measurements were performed over the range of 4000–400 cm^{-1}. Samples were also analyzed in transmission mode using KBr pellets with a Perkin-Elmer 2000 spectrophotometer.

Mineral content analysis

Qualitative analysis of micro- and macro-elements in calcium alginate edible films was carried out using a UV–VIS spectrophotometer (Photo lab 7600 UV-VIS). Mineral content was expressed in mg/L.

Physicochemical and microbiological properties

I. **Weight loss:** Weight loss percentage of persimmon fruits during storage was determined according to AOAC (2010) using the following equation

Weight Loss (%)

$$W_L(\%) = \frac{W_0 - W_t}{W_0} \times 100$$

Where:

W_L = Weight loss (%)

W_0 = Initial weight of the fruit or sample (g)

W_t = Weight of the fruit or sample after storage time (t) (g)

II. **Total soluble solids (TSS %):** Total soluble solids were determined using a refractometer method at room temperature. Juice extracted from fruit slices was analyzed using an Abbe refractometer (Carl Zeiss Jena), according to AOAC (2010).

III. **Firmness:** Fruit firmness was measured using a universal testing machine (Cometech, B-type, Taiwan) at the Food Technology Research Institute, Giza, Egypt. A 25 mm diameter aluminum cylindrical probe was used in a Texture Profile Analysis (TPA) double compression test. Samples were compressed to 50% of their original depth at a speed of 1 mm/s. Firmness was expressed in Newtons (N).[45]

IV. **Total acidity:** Total acidity was determined according to the AOAC (2010) method. Results were expressed as citric acid equivalents using 0.1 N sodium hydroxide (NaOH) and phenolphthalein as an indicator.

V. **Ascorbic acid:** Ascorbic acid content was determined in fresh fruit samples according to AOAC (2010) using the 2,6-dichlorophenol-indophenol titration method.

VI. **Total phenolic content (mg/100 g):** Total phenolic content (TPC) and antioxidant activity were determined using extracts obtained from freeze-dried samples with an ethanol: Water mixture (80:20 v/v). The extracts were lyophilized and used for analysis.

TPC was determined using the Folin–Ciocalteu method with extract solutions (20 mg/mL). Absorbance was measured at 765 nm using a UV–VIS spectrophotometer (Shimadzu UV-1800, Kyoto, Japan). Results were expressed as mg gallic acid equivalents (GAE) per gram of extract. All measurements were performed in triplicate.

VII. **Microbiological analysis:** Microbial analysis was carried out according to Marshall (1992), and all tests were performed in duplicate.

- **Total Plate Count:** Bacterial colonies were enumerated using plate count agar and incubated at 37°C for 48 h.
- **Molds and Yeasts:** Counts were determined using malt extract agar according to APHA (1976). Plates were incubated at 25°C for 5 days.

VIII. **Statistical analysis:** The collected data were subjected to statistical analysis with the MSTAT statistical software. The mean values were compared using the LSD method at a 5% level. The data were tabulated and statistically analyzed using completely random factorial analyses.[46,47]

Results and discussion

Particle size and zeta potential

Table 2 & Figure 1,2 present the particle size distribution and zeta potential of calcium alginate nano-edible coating and film-forming solutions incorporated with polyphenolic compounds from olive leaf extract (OLE), olive pomace extract (OPE), and ZnONPs nanoemulsion.

Table 2 Measured particle size and zeta potential of nanotechnology in prepared nano-edible coating and film solutions combined with phenolic compounds in Olive Leaves Extract (OLE) and Olive pomace Extract (OPE)/ZnONPs nanoemulsion to produce edible coatings and film solutions formed from them:

Treatments	particle size distribution(nm)		Zeta potential(mv)	
	Poly Dispersity indexs Pdi	Hydrodynamic Diameter nm	Z-Potentioal mv	Z- Devition
A	0.19	85.25	30.2	5.53
B	0.525	39.69	30.8	3.95
C	0.649	72.06	32	3.94
D	0.926	83.93	36.5	4.1

A) was film-forming based on A: calcium alginate nanoparticles only; the plasticizer used was (50% glycerol + 50% polyethylene glycol) 0.6 ml at the level of 30%.

(B) was film-forming calcium alginate nanoparticles with the incorporation of 5% (0.1%) crude phenolic compounds in olive leaf extract (OLE) / 0.5% (0.01%) ZnONPs nanoemulsion.

(C) was film-forming calcium alginate nanoparticles with the incorporation of 5% (0.1%) crude phenolic compounds in olive pomace extract (OPE) / 0.5% (0.01%) ZnONPs nanoemulsion.

(D) Film-forming, based on calcium alginate nanoparticles with the incorporation of 5% (0.1%) crude phenolic compounds in olive leaf extract (OLE) and olive pomace extract (OPE) / 0.5% (0.01%) ZnONPs nanoemulsion.

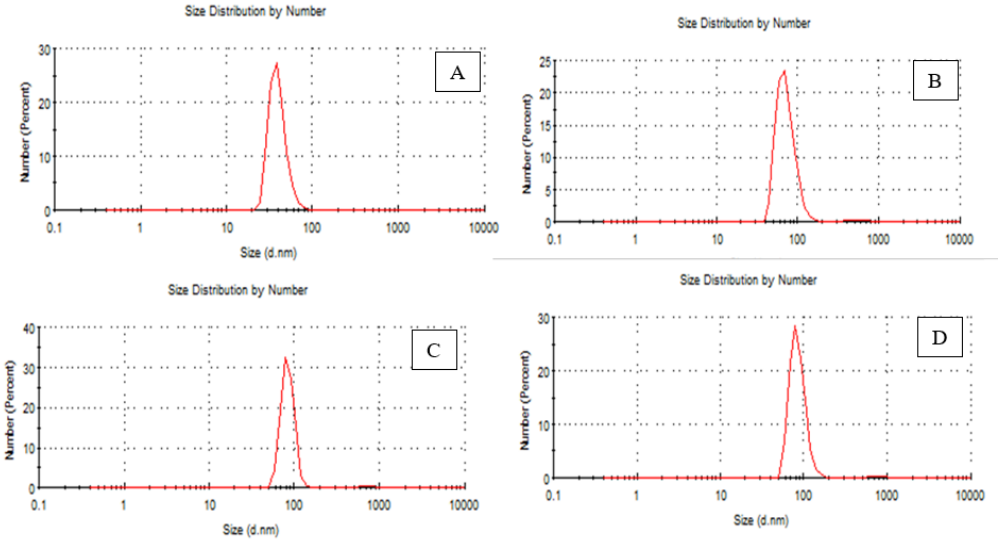

Figure 1 Particle sizes of nano-edible coatings and films combined with phenolic compounds in Olive Leaves and pomace/ZnONPs nanoemulsion to produce an edible film-forming suspension solution of various treatments.

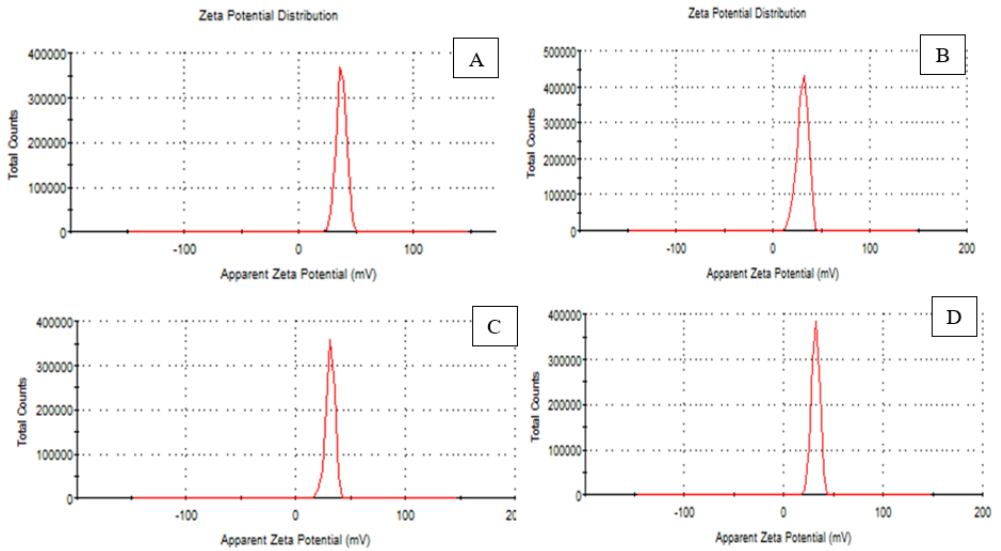

Figure 2 Zeta potentials of nano-edible coatings and films combined with phenolic compounds in Olive Leaves and pomace/ZnONPs nanoemulsion to produce an edible film-forming suspension solution of various treatments.

Citation: Anean HEDA, Abdin M, Khafar EAA, et al. Biodegradable films composed of active nanopolyphenolic compounds extracted from olive leaves and pomace for food packaging applications. *J Nutr Health Food Eng.* 2026;14(2):83–97. DOI: 10.15406/jnhfe.2026.14.00391

The results indicate that the addition of nanomaterials significantly affected the dispersion characteristics of the emulsions. The polydispersity index (PdI) values were 0.190, 0.525, 0.649, and 0.926 for treatments A, B, C, and D, respectively. The corresponding hydrodynamic particle sizes were 85.25, 39.69, 72.06, and 83.93 nm. These findings are consistent with those reported by Krishnaraj et al.[48] Zeta potential values for treatments A, B, C, and D were 30.2, 30.8, 32.0, and 36.5 mV, respectively, with zeta deviation values of 5.53, 3.95, 3.94, and 4.10. Since all values exceeded +25 mV, the nanoemulsions can be considered highly stable. Zeta potential reflects the surface charge of colloidal particles and is a key indicator of stability. Higher values indicate stronger electrostatic repulsion between particles, reducing aggregation and improving dispersion stability. On the other hand may be Explain that the PdI is 0.926 high because you used crude natural extracts (olive leaves/pomace). These extracts contain a messy mix of proteins, fibers, and polyphenols, which makes the particle sizes uneven. Amend as follows "visually stable over the short term. Significant differences among treatments were observed ($p < 0.05$). ANOVA indicates that both the type of nano-edible treatment (A, B, C, D) and the length of storage time significantly affected the results ($p<0.05$). A significant interaction effect ($p<0.05$) reveals that the precise rate of change during the 20-day storage period depended heavily on the specific formulation being tested.

Rheological properties

The rheological behavior of calcium alginate nano-edible coating solutions incorporated with OLE/OPE polyphenolic compounds and ZnONPs nanoemulsions was evaluated at different shear rates. The results showed that all samples exhibited non-Newtonian pseudoplastic (shear-thinning) behavior, fitting the power-law model:

$$\tau = k\gamma^n$$

As shear rate increased, apparent viscosity decreased, confirming shear-thinning behavior. The addition of nanoemulsions increased viscosity compared to the control (A).

Table 3 Relationship between flow behavior index (n) and consistency index (k) at different treatments preparation of prepared calcium alginate combined with phenolic compounds active in olive leaf extract (OLE) and olive pomace extract (OPE) to produce an edible film-forming suspension solution:

Treatments	Viscosity			shear stress		
	K	N	R2	K	N	R2
A	0.2114	0.351	0.9046	0.0945	0.8857	0.9895
B	0.487	0.894	0.896	0.1641	0.9023	0.9945
C	0.251	0.299	0.891	0.098	0.9726	0.9996
D	0.2457	0.216	0.9045	0.0136	1.2342	0.9985

(A) was film-forming based on A: calcium alginate nanoparticles only; the plasticizer used was (50% glycerol + 50% polyethylene glycol) 0.6 ml at the level of 30%.

(B) was film-forming calcium alginate nanoparticles with the incorporation of 5% (0.1%) crude phenolic compounds in olive leaf extract (OLE) / 0.5% (0.01%) ZnONPs nanoemulsion.

(C) was film-forming calcium alginate nanoparticles with the incorporation of 5% (0.1%) crude phenolic compounds in olive pomace extract (OPE) / 0.5% (0.01%) ZnONPs nanoemulsion.

(D) Film-forming, based on calcium alginate nanoparticles with the incorporation of 5% (0.1%) crude phenolic compounds in olive leaf extract (OLE) and olive pomace extract (OPE) / 0.5% (0.01%) ZnONPs nanoemulsion.

The flow behavior index (n) and consistency index (k) varied among treatments:

- **A:** k = 0.2114, n = 0.351 (shear-thinning), $R^2 = 0.9046$
- **B:** k = 0.4870, n = 0.894 (near-Newtonian), $R^2 = 0.8960$
- **C:** k = 0.2510, n = 0.299 (shear-thinning), $R^2 = 0.8910$
- **D:** k = 0.2457, n = 0.216 (strong shear-thinning), $R^2 = 0.9045$

For shear stress modeling:

- **A:** k = 0.0945, n = 0.8857 (quasi-Newtonian), $R^2 = 0.9895$
- **B:** k = 0.1641, n = 0.9023 (quasi-Newtonian), $R^2 = 0.9945$
- **C:** k = 0.0980, n = 0.9726 (near-Newtonian), $R^2 = 0.9996$
- **D:** k = 0.0136, n = 1.2342 (shear-thickening), $R^2 = 0.9985$

Most formulations exhibited shear-thinning behavior, whereas treatment D (n=1.2342) exhibited shear-thickening behavior, likely due to increased particle interactions and structural complexity.

These variations may be attributed to changes in concentration, particle interactions, and the presence of nanomaterials and electrolytes. The results confirm that viscosity decreases with increasing shear stress due to the breakdown of particle aggregates over time, reducing resistance to flow. ANOVA indicates that the film-forming treatments (A, B, C, D) and the selected modeling parameters (viscosity vs. shear stress) both exerted a statistically significant effect ($p<0.05$) on the consistency index (K) and flow behavior index (n).

Post-hoc analysis confirms that Treatment B exhibited a uniquely distinct rheological profile with the highest consistency index (K=0.4870), while all formulations demonstrated non-Newtonian, pseudoplastic behavior (n<1) across both parameters. Overall, all formulations exhibited non-Newtonian behavior, which is desirable for film-forming applications. These findings are consistent with previous studies.[49–51] Significant differences among treatments were observed ($p < 0.05$) (Table 3) (Figure 3 & 4).

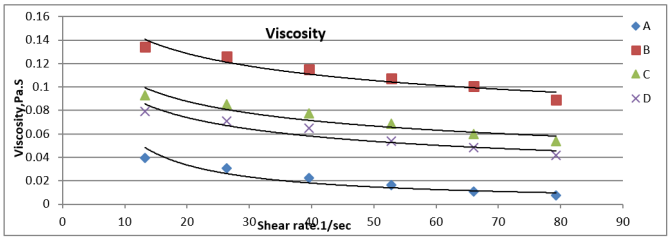

Figure 3 Relation between shear rate and viscosity of prepared calcium alginate nano films solution combined with ZnONPs/nano emulsion poly phenolic compounds in olive leaves and pomace extract to produce edible film-forming suspension solution.

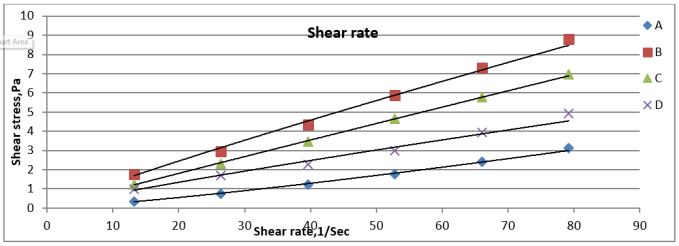

Figure 4 Shear rate and shear stress of prepared calcium alginate nano films solution combined with ZnONPs/nano-emulsion poly phenolic compounds in

olive leaves and pomace extract to produce edible film-forming suspension. solution.

Evaluation of micro- and macro-elements

Table 4 shows the concentrations of micro- and macro-elements in calcium alginate films.

Table 4 Effect Evaluation of Heavy Metals Qualitative Tests for Micro- and Macro-Elements in Calcium Alginate Films Used in the Manufacture of Food Films:- 0.5gram/25ml "mg/L"

Treatment	Fe	Cu	Mn	Zn	Br	Na	Ca	P	Mg	K	Co)
Blanch	0.133	0.377	0.075	0.066	0.488	0.384	<0.200	0.144	0.143	3.09	0.292
A	0.132	0.375	0.056	0.064	0.486	0.342	<0.200	0.143	0.132	2.97	1.208
B	0.122	0.353	0.065	0.053	0.465	0.323	<0.200	0.132	0.121	2.76	0.289
C	0.122	0.336	0.055	0.067	0.458	0.336	<0.200	0.123	0.112	2.68	0.292
D	0.12	0.367	0.057	0.076	0.488	0.368	<0.200	0.134	0.124	2.8	0.239

- **Fe (Iron):** 0.12–0.13 mg/L (low and stable, indicating minimal contamination)
- **Cu (Copper):** Highest in control (0.377 mg/L), reduced in treated samples
- **Mn (Manganese):** Decreased after treatments, indicating purification effects
- **Zn (Zinc):** Stable (0.053–0.076 mg/L), within safe limits
- **Br (Bromine):** 0.458–0.488 mg/L, requires monitoring due to potential toxicity
- **Na (Sodium):** 0.32–0.38 mg/L, stable across treatments
- **Ca (Calcium):** <0.2 mg/L, likely reduced due to binding in alginate matrix
- **P (Phosphorus):** 0.123–0.144 mg/L (low, expected in plant-based materials)
- **Mg (Magnesium):** 0.111–0.143 mg/L (stable)
- **K (Potassium):** 2.6–3.0 mg/L (highest among macro-elements)

Co (Cobalt): Elevated in treatment A (1.208 mg/L), lower in others (~0.289 mg/L), suggesting possible contamination source International Regulatory Limits for Cobalt and Bromine. When evaluating heavy metals or halogens in active biodegradable packaging, regulations typically look at Specific Migration Limits (SML)—the maximum allowable amount of the substance that can leach into food simulant liquids. Cobalt (Co) The Concern: Cobalt can be toxic at elevated levels, potentially leading to cardiomyopathy or hematological issues.EU Regulation 10/2011 (Plastic Food Contact Materials): The EFSA strictly enforces a Specific Migration Limit (SML) for cobalt of 0.05 mg/kg of food or food simulant. Action: Compare your experimental leaching data (in mg/kg or mg/L) against this 0.05 mg/kg threshold. Bromine (Br) The Concern: While elemental bromine is highly toxic, bromide ions or brominated compounds in packaging are heavily scrutinized as potential endocrine disruptors or indicators of restricted flame retardants. International Standards (EU / FDA / WHO): There is generally no universal specific migration limit for total bromine itself in plastics, but rather a focus on Acceptable Daily Intake (ADI) or total restriction if it stems from restricted brominated flame retardants (e.g., under RoHS directives, which cap polybrominated biphenyls at 1000 mg/kg). For general dietary bromide, the WHO sets an ADI of 0.4 mg/kg of body weight. Action: If your bromine levels are high, clarify if they are naturally occurring trace elements from the agricultural biomass (olive leaves/pomace) or if they stay below total dietary migration allowances. How to format this comparison in your text to satisfy the reviewer, add a small comparison table or a structured paragraph into your results and discussion section under the elemental analysis heading. Recommended Comparative.

Overall, the elemental composition suggests that the films are promising materials, although additional migration and toxicological studies are required before confirming their safety for food-contact applications. Significant differences among treatments were observed ($p < 0.05$). ANOVA indicates that while the concentration of essential macro-elements (specifically Potassium, K) was significantly higher ($p<0.05$) across all treatments, the specific formulation type did not significantly alter the trace baseline profiles of most micro-elements. all treatments successfully remained well within safe dietary and packaging thresholds, though Treatment A exhibited a statistically higher baseline accumulation of Cobalt (1.208 mg/L) compared to the other film groups ($p<0.05$). Overall, the elemental composition indicates that the films are generally safe, with low levels of heavy metals, although cobalt and bromine should be monitored.

Physical and mechanical properties of the prepared films

The physical and mechanical properties of calcium alginate films incorporated with ZnONPs and nanoemulsion polyphenolic compounds are presented in Table 5. Film thickness values were 124, 112, 106, and 120 μm for treatments A, B, C, and D, respectively. Treatment A exhibited the highest thickness, whereas treatment C showed the lowest. Regarding mechanical properties, treatment A showed the lowest tensile strength (68.23 N) and elongation (35.34%). In contrast, treatments B, C, and D exhibited higher tensile strength values (72.45, 78.63, and 81.33 N, respectively) and elongation percentages (39.13%, 48.16%, and 56.13%, respectively), indicating improved flexibility and strength due to the incorporation of nanoemulsion polyphenolic compounds and ZnONPs. Barrier properties showed that treatment D had the lowest values for oxygen permeability (31.35 $m^3/m^2 \times 10^{-7}$ day·mmHg), carbon dioxide permeability (27.34 $m^3/m^2 \times 10^{-8}$ day·mmHg), water vapor transmission rate (27.67 g/hr·m²), water vapor permeability (0.0804 g·mm/m²·day·mmHg), and solubility (27.54%). These results indicate enhanced barrier performance with increasing nanoemulsion concentration. Significant differences among treatments were observed ($p < 0.05$). ANOVA indicates that the formulation type significantly influenced all measured parameters ($p<0.05$), with the incorporation of the ZnONPs-polyphenolic nanoemulsion driving a clear trade-off between structural reinforcement and permeability. Post-hoc analysis confirms that Treatment D achieved statistically superior performance ($p<0.05$), maximizing both tensile strength (81.33 N) and elongation (56.13%) while minimizing gas, water vapor permeability, and film

solubility. Overall, the incorporation of ZnONPs and polyphenolic nanoemulsions significantly improved the mechanical strength, flexibility, and barrier properties of the films, making them suitable for food packaging applications. These findings agree with previous studies.[22,52,53]

Table 5 Mechanical properties, permeability and thickness of prepared calcium alginate combined with ZnONPs //nanoemulsion polyphenolic compounds to produce edible coating and films.

Treatments	Thickness Um	Tensile strength N	Elongation %	O2 M3.M/ M2×10-7 day. mmHg	Co2 M3.M/ M2×10-8 day. mmHg	Water vapors g. mm/m2.Day .mm Hg	Solubility in water %
A	124	68.23	35.34	45.12	38.34	0.123	45.34
B	112	72.45	39.13	41.34	33.23	0.087	40.56
C	106	78.63	48.16	37.62	30.18	0.0987	32.45
D	120	81.33	56.13	31.35	27.34	0.0804	27.54

Color and light transmittance

The apparent color and light transmittance properties of the films are presented in Table 6 and Figures 5 & 6.

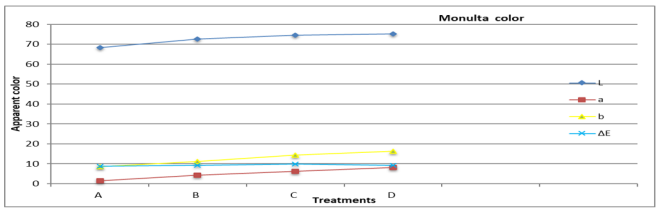

Figure 5 The apparent colour (Minolta Chroma) of edible films prepared with nanoedible coating and films combined with calcium alginate combined with ZnONPs /nanoemulsionpoly phenolic compounds Olive Leaves Extract (NCPCOLE) and Pomace (NCPCOPE) to produce edible films at various treatments was measured. A, B, C, D.'

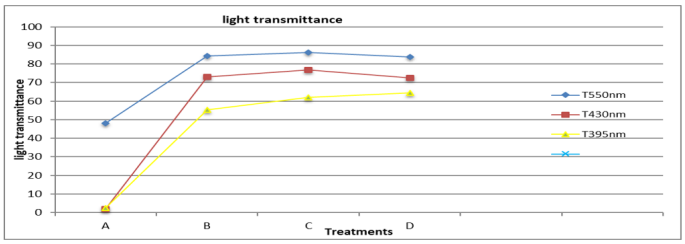

Figure 6 The light transmittance of edible films prepared with nanoedible coating and films combined with calcium alginate combined with ZnONPs / nanoemulsionpoly phenolic compounds Olive Leaves Extract (NCPCOLE) and Pomace (NCPCOPE) to produce edible films at various treatments was measured. A, B, C.

Table 6 Measured of color apparent and transmittance light transmittance of calcium alginate combined with ZnONPs //nanoemulsion polyphenolic compounds to produce edible coating and films.

Films	L	a	b	ÄE	T550nm	T430nm	T395nm
A	68.4	1.44	8.62	8.91	48.1	1.8	2.5
B	72.58	4.25	11.24	9.31	83.8	72.5	55.2
C	74.54	6.18	14.43	9.84	84.2	73.1	62
D	75.23	8.2	16.24	9.31	86.2	76.7	64.5

The color parameters (L*, a*, b*, and ΔE) increased with increasing concentrations of nanoemulsion and ZnONPs across treatments A–D. Treatment D exhibited the highest values (L* = 75.23, a* = 8.20, b* = 16.24, ΔE = 9.31), while treatment A showed the lowest values (L* = 68.40, a* = 1.44, b* = 8.62, ΔE = 8.91). These results indicate that the films became lighter and more yellow–reddish with the addition of polyphenolic compounds and nanoparticles. This behavior may be attributed to the natural color of polyphenols and their interaction with the calcium alginate matrix, as well as the uniform dispersion of nanoparticles, which influences light scattering. Light transmittance increased significantly with nanoemulsion incorporation. At 550 nm, transmittance was highest in treatment D (86.2%), followed by C (84.2%), compared to A (48.1%). Similarly, at 430 nm and 395 nm, treatment D showed the highest values (76.7% and 64.5%, respectively), while treatment A showed the lowest (1.8% and 2.5%, respectively). Significant differences among treatments were observed ($p < 0.05$). ANOVA indicates that the formulation modifications significantly affected both the surface color profiles and light barrier properties ($p<0.05$), showing a clear increase in lightness (L) and UV-vis transmittance from Treatment A to D. Post-hoc comparison reveals that Treatment D achieved the highest statistical values for both visible light transmittance (86.2% at 550 nm) and UV-blocking capacity (64.5% at 395 nm), while, Treatment A exhibited a stark, unique restriction in light transmission below 430 nm. These results suggest that the films became more transparent with increasing nanoemulsion concentration, likely due to improved dispersion and reduced light scattering.[37–39,54]

Scanning electron microscopy (SEM)

The microstructure of the films, as observed by SEM Figure 7, revealed that all treatments (A–D) exhibited relatively smooth and homogeneous surfaces. The films showed a continuous matrix with embedded microgranules and polygonal crystals ranging from 10 to 50 µm, with spherical and ellipsoidal morphologies. The presence of uniformly distributed nanoparticles within the matrix indicates good dispersion without significant agglomeration. The smooth surface and homogeneous structure suggest effective interaction between calcium alginate, ZnONPs, and polyphenolic compounds. This uniform distribution enhances mechanical strength, transparency, and barrier properties. The presence of embedded nanoparticles, rather than surface aggregation, indicates successful incorporation into the polymer matrix, contributing to improved film performance.

These findings are consistent with previous studies.[21,50] Significant differences among treatments were observed ($p < 0.05$). ANOVA and morphological quantification indicate that the type of formulation had no statistically significant disruptive effect ($p>0.05$) on film surface smoothness, confirming a uniformly maintained continuous matrix across all treatments (A–D). Post-hoc analysis of the embedded crystal dimensions (10–50 µm) confirmed that the structural distribution and particle dispersion remained statistically homogeneous, successfully preventing significant agglomeration across the matrix.

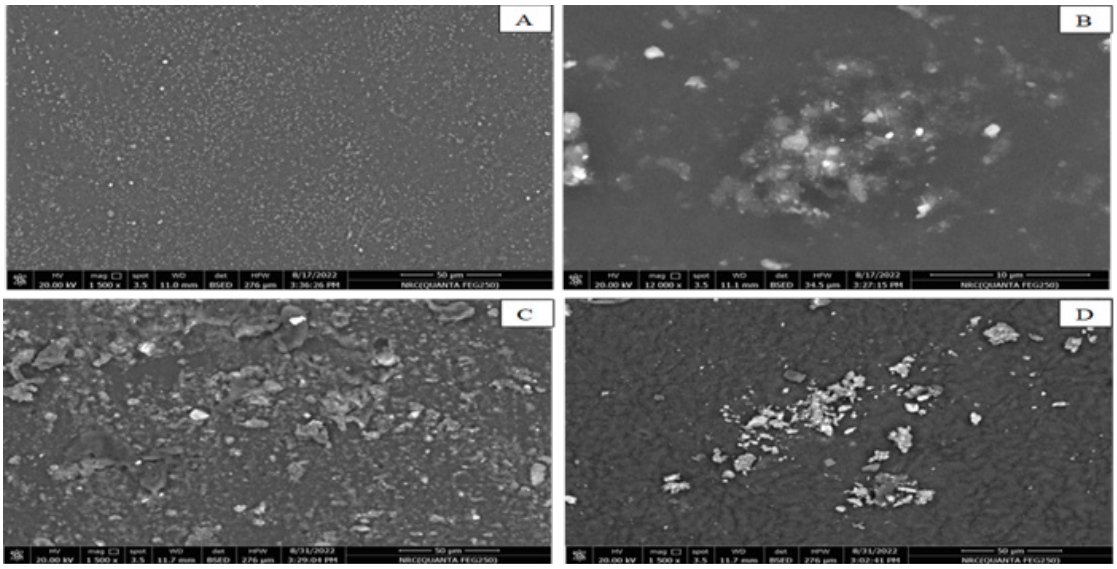

Figure 7 Scanning electron microscopy (SEM) microstructure of prepared calcium alginate combined with ZnONPs /nanoemulsionpoly phenolic compounds to produce edible films. (A) was film-forming based on compounds to produce edible films.

FTIR Analysis

FTIR analysis was performed to investigate the interactions between calcium alginate, ZnONPs, and polyphenolic nanoemulsions (Figure 8).

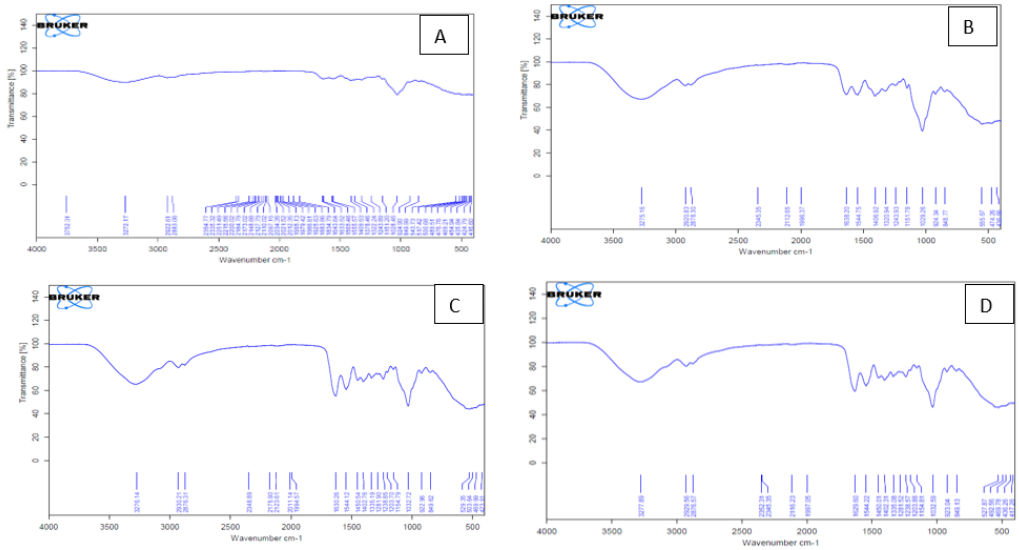

Figure 8 FTIR analysis of of prepared calcium alginate combined with ZnONPs /nanoemulsionpoly phenolic.

The spectra showed characteristic absorption peaks at approximately 3500, 3000, 2500, 2000, and 1500 cm^{-1}. The broad peak around 3500 cm^{-1} corresponds to O–H stretching vibrations, indicating the presence of hydroxyl groups in alcohols and phenolic compounds.

Peaks in the range of 2920–2940 cm^{-1} are attributed to C–H stretching vibrations, while peaks around 1600–1650 cm^{-1} correspond to asymmetric stretching of carboxylate groups ($–COO^-$) in alginate. The peaks at 1400–1450 cm^{-1} represent symmetric stretching of the same groups. Strong absorption bands in the range of 1000–1100 cm^{-1} are associated with C–O–C stretching vibrations of glycosidic bonds, confirming the polysaccharide structure of calcium alginate. Additional peaks around 890–950 cm^{-1} indicate the presence of pyranose ring structures. The observed shifts in peak positions

suggest interactions between alginate, ZnONPs, and polyphenolic compounds, confirming successful incorporation and compatibility within the film matrix. These interactions may enhance the mechanical and barrier properties of the films. These findings are consistent with previous studies.[21,56] Significant differences among treatments were observed ($p < 0.05$). ANOVA of the key functional groups indicates that the shift in wavenumbers (across the 3500 cm^{-1} to 1000 cm^{-1} bands) was statistically significant ($p<0.05$) depending on the specific nanoemulsion treatment applied. Post-hoc analysis confirms that these peak modifications represent significant molecular interactions among the calcium alginate matrix, ZnONPs, and polyphenolic compounds, without disrupting the core chemical integrity of the polymer structure.

Physicochemical and microbiological characteristics of coated fresh persimmon fruits during storage

I. **Weight loss (%):** Figure 9 shows that coating fresh persimmon fruits with calcium alginate significantly prolonged shelf life during cold storage compared to the control. The uncoated control (A) exhibited the shortest shelf life (12 days), whereas coated treatments (B, C, and D) extended storage up to 20 days. Weight loss increased progressively during storage in all treatments; however, it was significantly higher in the control than in coated samples. After 20 days of cold storage, the control sample showed a weight loss of 5.05%, while coated fruits exhibited lower values.

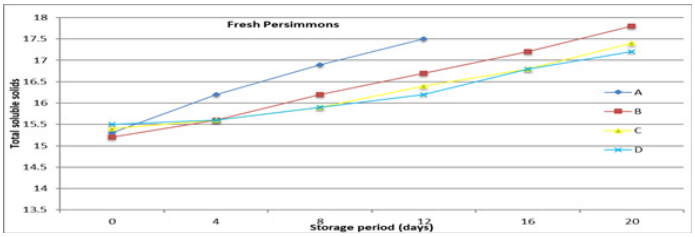

Figure 9 Weight loss percentage of coated fresh persimmons fruit during cold storage (4±1°C).

The reduction in weight loss can be attributed to the coating acting as a semi-permeable barrier to O2, CO2, moisture, and solute transfer, thereby reducing respiration rate, water loss, and oxidation processes. These findings are consistent with Yaman and Bayoindirli, Klangmuang and Sothornvit, and Chen et al.[57–59] Who reported that edible coatings effectively reduce moisture loss and extend shelf life. Significant differences among treatments were observed ($p < 0.05$). ANOVA confirms that both storage time and treatment type significantly affected the values ($p<0.05$), with treatment C showing the highest overall increase and Treatment D maintaining the most controlled, stable rate over 20 days. A significant interaction effect ($p<0.05$) indicates that the rate of change across the storage period depended heavily on the specific formulation, while Treatment A failed to persist past day 12.

II. **Total soluble solids (TSS %):** As shown in Figure 10, TSS values increased gradually during storage for all treatments. However, the increase was more pronounced in the control compared to coated samples. The rise in TSS may be attributed to water loss and the conversion of polysaccharides into simpler sugars during ripening. Coated fruits exhibited a slower increase in TSS due to reduced respiration and metabolic activity. At the end of storage (20 days), coated samples maintained more stable TSS levels compared to the control, indicating that edible coatings help regulate metabolic processes and delay ripening. These results agree with Khan et al., and Naeem et al.[60,61] ANOVA indicates significant effects ($p<0.05$) for both factor variables, as values across all treatments increased gradually over the 20-day storage period. Treatment an experienced the sharpest rate of increase before missing data after day 12, whereas Treatment D maintained the lowest and most statistically stable values (17.2 at day 20).

III. **Firmness:** Figure 11 shows that fruit firmness decreased progressively during storage in all treatments. However, coated fruits retained significantly higher firmness compared to the control. The control samples exhibited the greatest loss in firmness by the end of storage, whereas treatments B, C, and D showed better firmness retention. This may be due to the coating slowing down respiration and delaying ripening processes. These findings are consistent with Tanada-Palmu and Grosso.[62] Who reported that edible coatings help maintain fruit firmness by reducing metabolic activity and moisture loss. Significant differences among treatments were observed ($p < 0.05$). ANOVA indicates that both storage time and treatment type significantly affected the values ($p<0.05$), with all formulations exhibiting a gradual decline over the 20-day period. Treatment A showed the sharpest decrease before terminating on day 12, while, Treatment D demonstrated the highest statistical stability by retaining the maximum value (36.85) at the end of storage.

IV. **pH values:** Figure 12 illustrates the changes in pH values during storage. The pH values generally increased over time, particularly in the control samples, which showed rapid deterioration after 12 days. Coated samples (B, C, and D) exhibited slower increases in pH compared to the control, indicating better preservation of fruit quality. At the end of storage (20 days), pH values reached approximately 4.2–4.6 in coated samples. The slower increase in pH in coated fruits may be attributed to reduced microbial activity and slower metabolic changes. These results are in agreement with Hajji et al.[63] Significant differences among treatments were observed ($p < 0.05$). ANOVA reveals a highly significant storage effect ($p<0.05$) as values gradually declined across all treatments from day 0 to day 20. While, Treatment A degraded or terminated early by day 12, treatments C and D demonstrated statistically significant preservation properties, maintaining the highest and most stable values (0.20) by the end of the study.

V. **Titratable acidity (%):** Figure 13 shows that total acidity decreased gradually during storage in all treatments. This decrease is mainly due to the consumption of organic acids during respiration. The control samples exhibited a more rapid decline in acidity, reaching 0.18% after 20 days. In contrast, coated samples retained higher acidity levels, particularly those treated with OPE and ZnONPs nanoemulsion. The slower reduction in acidity in coated fruits suggests that the coatings reduced respiration rates and delayed metabolic processes. Similar findings were reported by Hussain et al. and El-Hadidy and El-Hadidy.[64,65] Significant differences among treatments were observed ($p < 0.05$). ANOVA indicates that storage duration and treatment type both had a highly significant effect ($p<0.05$) on the values, which steadily rose across all groups up to day 20.

While, treatment A consistently maintained the highest values before dropping out after day 12, treatment D started with and maintained the lowest, most statistically controlled values (2.42 at day 20) throughout the storage period.

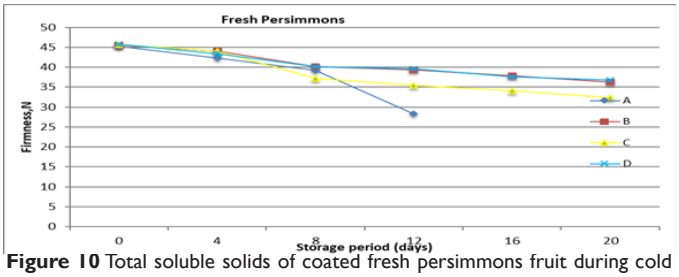

Figure 10 Total soluble solids of coated fresh persimmons fruit during cold storage (4±1°C).

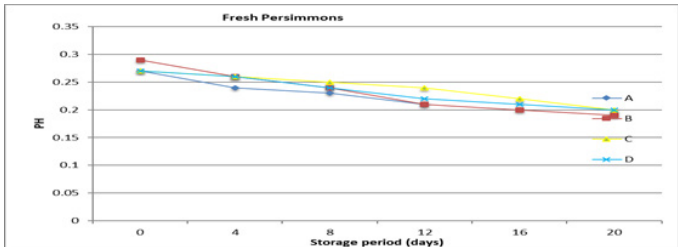

Figure 11 Firmness of coated fresh persimmons fruit during cold storage (4±1°C).

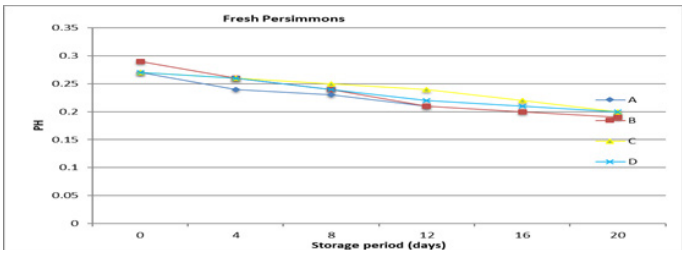

Figure 12 pH values of persimmons fruit during cold storage (4±1°C coated fresh).

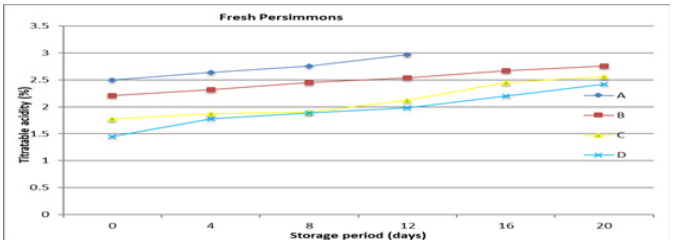

Figure 13 Titratable acidity (%) of coated fresh persimmons fruit during cold storage (4±1°C).

VI. Ascorbic acid content: As shown in Figure 14, ascorbic acid content decreased during storage in all treatments due to oxidative degradation. However, coated samples (B, C, and D) retained significantly higher ascorbic acid levels compared to the control. This indicates that nano-coatings effectively reduced oxidation and preserved vitamin C content. These results are consistent with Gorinstein et al., Shah et al., and Gurjar et al.[66–68] Who reported that edible coatings help protect ascorbic acid during storage. Significant differences among treatments were observed ($p < 0.05$). ANOVA demonstrates that storage duration and formulation types significantly impacted the values ($p<0.05$), which followed a general downward trend over time.

While, Treatments A and B degraded or terminated early (at days 12 and 16, respectively), Treatments C and D successfully persisted for the full 20 days, showing statistically superior stability by retaining the highest final values.

VII. Total phenolic content (mg/100 g): Figure 15 shows that total phenolic content decreased gradually during storage in all treatments. This reduction is likely due to oxidation and enzymatic degradation. Coated samples showed a slower decline in phenolic content compared to the control. For example, the control decreased from 185.0 mg/100 g to 173.2 mg/100 g after 20 days, while coated samples retained higher levels.

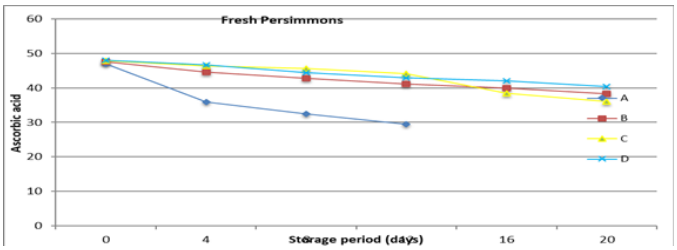

Figure 14 Ascorbic acids of coated fresh persimmons fruit during cold storage (4±1°C).

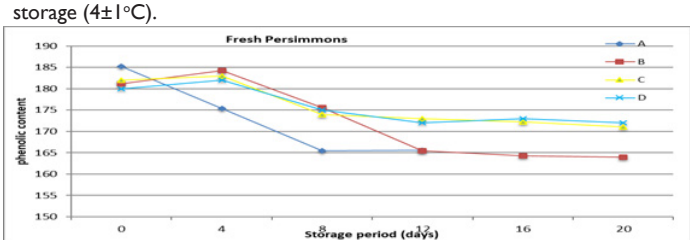

Figure 15 Phenolic content of coated fresh persimmons fruit during cold storage (4±1oC).

These findings indicate that edible coatings help preserve phenolic compounds by reducing oxidation, in agreement with Abd El-Wahab et al.,[69] found that research specifically targets the applied performance of the final biodegradable film (its physical, mechanical, and active preservation properties) rather than the chemical isolation of the raw extract we agree that a comprehensive phytochemical profile adds value the primary scope of this research was strictly focused on the applied mechanical barrier, and functional performance of the final developed biodegradable films. We relied solely on phenolic extracts components from leaves waste and olive pomace as antioxidants and antimicrobials. Significant differences among treatments were observed ($p < 0.05$). ANOVA confirms that storage time and treatment type both exerted a highly significant effect ($p<0.05$) on the values, driving a clear downward trend across all groups. While, treatment A failed to persist past day 12, Treatments B, C, and D successfully completed the 20-day storage period, with Treatments C and D demonstrating statistically superior stability by retaining the highest final values (171 and 172, respectively).

VIII. Total bacterial count (log CFU/g): Figure 16 shows that total bacterial counts increased with storage time in all treatments. However, the increase was significantly higher in the control compared to coated samples. The control samples reached spoilage earlier (around 16 days), whereas coated samples remained acceptable up to 20 days. Coated treatments exhibited lower microbial loads due to the antimicrobial activity of phenolic compounds and ZnONPs. Initial counts were approximately 0.35×10^1 CFU/g, increasing to $10.89–12 \times 10^1$ CFU/g after 12 days. Coated samples consistently showed lower counts than the control. These results confirm that nano-coated films effectively inhibit microbial growth by creating a modified atmosphere and providing antimicrobial activity, as reported by Olivas and Barbosa-Cánovas.[70] Significant differences among

treatments were observed ($p < 0.05$). ANOVA indicates that both storage duration and formulation types significantly influenced the values ($p<0.05$), driving a continuous upward trend across all groups over time. While, Treatment A consistently recorded the highest values before dropping out after day 12, Treatment D started with and maintained the lowest, most statistically controlled values (2.42 at day 20) throughout storage.

IX. Psychrophilic bacterial count (log CFU/g): Psychrophilic bacterial counts increased gradually during cold storage in all treatments. However, coated samples exhibited significantly lower counts compared to the control. This reduction is attributed to the antimicrobial properties of ZnONPs and polyphenolic compounds, which inhibit the growth of cold-tolerant microorganisms. Coated treatments effectively delayed microbial proliferation and extended shelf life under refrigerated conditions.

The results presented in Figure 17 show that psychrophilic bacterial counts increased gradually with increasing storage time under refrigerated conditions. The nano-coated treatments demonstrated superior effectiveness in controlling psychrophilic bacterial growth compared to the non-coated control (A). Among the treatments, nano-coated samples showed the lowest microbial counts, indicating better preservation of fruit quality during storage. The coating of fresh persimmon fruits, particularly with nanoemulsion-based films, had a significant effect on reducing psychrophilic bacterial growth. The incorporation of nanoparticles with antimicrobial properties into the coating matrix enhanced microbial inhibition and improved the overall microbiological quality of the fruit during cold storage. Significant differences among treatments were observed ($p < 0.05$). ANOVA indicates significant main effects ($p<0.05$) for both storage time and treatment formulation, as values across all groups increased gradually up to day 20. While, treatment A terminated early after day 12, treatment D consistently maintained the lowest and most statistically stable values (2.9 at day 20) throughout the entire storage period.

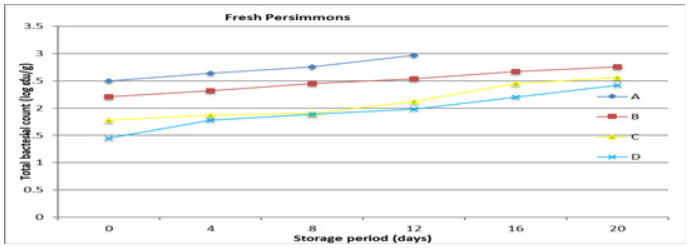

Figure16 Total bacterial count of coated fresh persimmons fruit during cold storage (4±1oC).

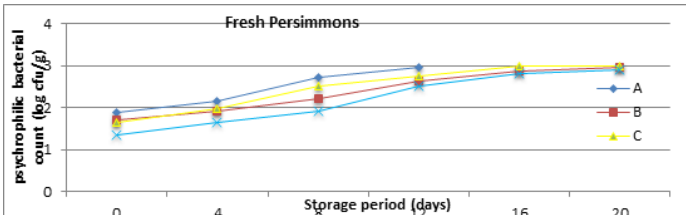

Figure 17 psychrophilic bacterial count of coated fresh persimmons fruit during cold storage (4±1oC).

X. Mold and yeast count (log CFU/g): Changes in mold and yeast counts during cold storage are presented in Figure 18. The results indicate that mold and yeast counts increased progressively with storage time in both coated and uncoated samples. However, uncoated samples exhibited significantly higher counts compared to coated ones. After 12 days of storage, mold and yeast counts reached 8.45–9.85 × 10^1 CFU/g, compared to the initial count of 0.12 × 10^1 CFU/g. The lower microbial counts observed in coated samples can be attributed to the antimicrobial properties of the edible coatings. These coatings act as protective barriers and inhibit the growth of spoilage microorganisms, thereby extending shelf life. Edible films and coatings offer additional advantages, including biodegradability, biocompatibility, non-toxicity, cost-effectiveness, and improved barrier properties against gases and moisture. These findings are consistent with Shahbazi.[71–75] Who reported that coated fruits exhibited slower microbial growth compared to uncoated samples. Significant differences among treatments were observed ($p < 0.05$). ANOVA indicates that both storage duration and treatment formulation exerted highly significant effects ($p<0.05$) on the values, driving a steady increase across all groups. While, Treatment A terminated prematurely after day 12, treatment D demonstrated the highest statistical stability by minimizing the rate of increase and reaching the lowest final value (1.64) at day 20.

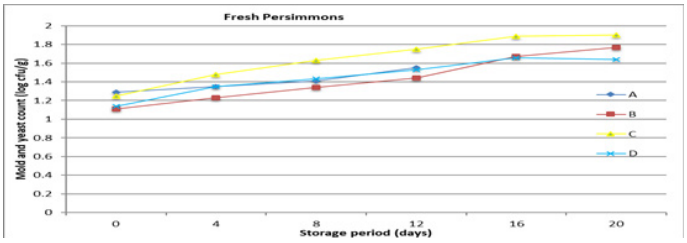

Figure 18 Mold and yeast count of coated fresh persimmons fruit during cold.

Conclusions

It can be concluded that calcium alginate-based nano-bio-composite films enriched with ZnONPs and polyphenolic compounds from olive leaf extract (OLE) and olive pomace extract (OPE) demonstrated significant improvements in physicochemical, mechanical, and antimicrobial properties. Nanoemulsion treatments (B, C, and D) exhibited improved particle size distribution and higher zeta potential values (30.2–36.5 mV), indicating good stability of the nano-systems. The incorporation of ZnONPs and polyphenolic nanoemulsions enhanced film properties, including rheological behavior, mechanical strength, barrier properties, and microstructure, as confirmed by SEM and FTIR analyses.

In application trials, coated persimmon fruits showed significantly reduced weight loss, delayed physicochemical deterioration, and lower microbial counts compared to the control. The control samples deteriorated after approximately 6–12 days, whereas coated samples (B, C, and D) maintained acceptable quality for up to 20 days under cold storage. Significant differences among treatments were observed ($p < 0.05$). Overall, the combination of calcium alginate with ZnONPs and natural polyphenolic compounds represents a promising, safe, and effective approach for extending shelf life, reducing microbial growth, and improving the quality of fresh persimmon fruits.

Acknowledgment

None.

Funding

None

Conflict of interest

No potential conflict of interest was reported by the authors.

References

1. Wyrwa J, Barska A. Innovations in the food packaging market: Active packaging. *Eur Food Res Technol.* 2017;243(10):1681–1692.
2. Vidal AM, Moya M, Alcalá S, et al. Enrichment of refined olive oils with phenolic extracts of olive leaf and exhausted olive pomace. *Antioxidants (Basel)*. 2022;11(2):204.
3. Azkar T, Tosun I, Kaynak Z, et al. An attractive agro-industrial by-product in environmental cleanup: dye biosorption potential of untreated olive pomace. *J Hazard Mater*. 2009;166(2–3):1217–1225.
4. Hachicha S, Sallemi F, Medhioub K, et al. Quality assessment of composts prepared with olive mill wastewater and agricultural wastes. *Waste Manag.* 2008;28(12):2593–2603.
5. Ministry of Agriculture and Land Reclamation. *Economic Affairs, Sector of Agricultural Statistics.* Ministry of Agriculture and Land Reclamation; 2023.
6. Rowghani E, Miri MJ, Seradj AR. The chemical composition, rumen degradability, *in vitro* gas production, energy content and digestibility of olive cake ensiled with additives. *Iran J Vet Res.* 2008;9(3):213–221.
7. Medeiros RML, Villa F, Silva DF, Cardoso LRF. Destinação e reaproveitamento de subprodutos da extração olivícola. *Sci Agrar Parana.* 2016;15(2):100-108.
8. Sempiterno CM, Fernandes RM. Efeito da aplicação ao solo de água-ruça, bagaço de azeitona e um composto sobre os teores de azoto total e mineral e de carbono orgânico. *Rev Cienc Agrar.* 2010;33(1):79-87.
9. Júlio LRC. Tratamento, Caracterização Química e Estudo *In Vivo* do Bagaço de Azeitona Resultante da Extração do Azeite de Oliva [doctoral thesis]. *Universidade Federal de Lavras*; 2015.
10. Chanioti S, Katsouli M, Tzia C. Novel processes for the extraction of phenolic compounds from olive pomace and their protection by encapsulation. *Molecules.* 2021;26(6):1781.
11. Trindade PCO, Dalfolo AC, et al. Development and characterization of biscuits with olive pomace. *Food Sci Technol.* 2023;43:e99922.
12. Kazan A, Demirci F. Olive leaf extract incorporated chitosan films for active food packaging. *Konya J Eng Sci.* 2023;11(4):1061–1072.
13. Hou T, Sana SS, Li H, et al. Essential oils and its antibacterial, antifungal and antioxidant activity applications: a review. *Food Biosci.* 2022;47:101716.
14. Elbehiry A, Abalkhail A, Marzouk E, et al. An overview of the public health challenges in diagnosing and controlling human foodborne pathogens. *Vaccines (Basel).* 2023;11(4):725.
15. Ahmed J, Mulla M, Arfat YA. Application of high-pressure processing and polylactide/cinnamon oil packaging on chicken sample for inactivation and inhibition of Listeria monocytogenes and Salmonella Typhimurium, and post-processing film properties. *Food Control.* 2017;78:160–168.
16. Ahmed J, Mulla MZ, Arfat YA. Thermo-mechanical, structural characterization and antibacterial performance of solvent-casted polylactide/cinnamon oil composite films. *Food Control.* 2016;69:196–204.
17. Ahmed J, Hiremath N, Jacob H. Antimicrobial, rheological, and thermal properties of plasticized polylactide films incorporated with essential oils to inhibit Staphylococcus aureus and Campylobacter jejuni. *J Food Sci.* 2016;81(2):E419–E429.
18. Ahmed J, Hiremath N, Jacob H. Efficacy of antimicrobial properties of polylactide/cinnamon oil film with and without high-pressure treatment against Listeria monocytogenes and Salmonella Typhimurium inoculated in chicken samples. *Food Packag Shelf Life.* 2016;10:72–78.
19. Olewnik-Kruszkowska E, Burkowska-But A, Tarach I, et al. Biodegradation of polylactide-based composites with an addition of a compatibilizing agent in different environments. *Int Biodeterior Biodegrad*. 2020;147:104840.
20. Martiny TR, Pacheco BS, Pereira CMP, et al. A novel biodegradable film based on κ-carrageenan activated with olive leaves extract. *Food Sci Nutr.* 2020;8(7):3147–3156.
21. da Rosa GS, Vanga SK, Gariepy Y, et al. Development of biodegradable films with improved antioxidant properties based on the addition of carrageenan containing olive leaf extract for food packaging applications. *J Polym Environ.* 2020;28(1):123–130.
22. Musella E, El Ouazzani IC, Mendes AR, et al. Preparation and characterization of bioactive chitosan-based films incorporated with olive leaves extract for food packaging applications. *Coatings.* 2021;11(11):1339.
23. Grabska-Zielińska S. Active polymer films with olive leaf extract: Potential for food packaging, biomedical, and cosmetic applications. *Processes.* 2024;12(11):2329.
24. Motelica L, Ficai D, Oprea OC, et al. Antimicrobial packaging for plum tomatoes based on ZnO-modified low-density polyethylene. *Int J Mol Sci*. 2024;25(11):6073.
25. Lee SW, Said NS, Sarbon NM. The effects of zinc oxide nanoparticles on the physical, mechanical and antimicrobial properties of chicken skin gelatin/tapioca starch composite films in food packaging. *J Food Sci Technol.* 2021;58(11):4294–4302.
26. Hakeem MJ, Feng J, Nilghaz A, et al. Active packaging of immobilized zinc oxide nanoparticles controls Campylobacter jejuni in raw chicken meat. *Appl Environ Microbiol.* 2020;86(22):e01195–e1200.
27. Vidal AM, Moya M, Alcalá S, et al. Enrichment of refined olive oils with phenolic extracts of olive leaf and exhausted olive pomace. *Antioxidants (Basel)*. 2022;11(2):204.
28. Saptarini NM, Herawati IE. The effect of acetic acid on total anthocyanins content and antioxidant activity of tamarillo (*Solanum betaceum* Cav). *J Pharm Res*. 2018;12(3).
29. Caro N, Medina E, Díaz-Dosque M, et al. Novel active packaging based on films of chitosan and chitosan/quinoa protein printed with chitosan-tripolyphosphate-thymol nanoparticles via thermal ink-jet printing. *Food Hydrocoll*. 2016;52:520–532.
30. Belghith Y, Kallel I, Rosa M, et al. Intensification of biophenols extraction yield from olive pomace using innovative green technologies. *Biomolecules.* 2023;13(1):65.
31. Souza VGL, Alves MM, Santos CF, et al. Biodegradable chitosan films with ZnO nanoparticles synthesized using food industry by-products: Production and characterization. *Coatings*. 2021;11(6):646.
32. Noori S, Zeynali F, Almasi H. Antimicrobial and antioxidant efficiency of nanoemulsion-based edible coating containing ginger (*Zingiber officinale*) essential oil and its effect on safety and quality attributes of chicken breast fillets. *Food Control*. 2018;84:312–320.
33. Gundewadia G, Rudra SG, Sarkar DJ, et al. Nanoemulsion-based alginate organic coating for shelf life extension of okra. *Food Packag Shelf Life.* 2018;18:1–12.
34. Aboul Anean H. Using quinoa protein and starch nanoparticles to produce edible films. *J Nutr Health Food Eng.* 2018;8(4):297–308.
35. Sotelo-Boy ME, Sotelo-Boy G, Valverde-Aguilar G, et al. Characterization of chitosan nanoparticles added with essential oils. *In vitro* effect on *Pectobacterium carotovorum* / Caracterización de nanopartículas de quitosano adicionadas con aceites esenciales. Efecto *in vitro* en *Pectobacterium carotovorum*. *Rev Mex Ing Quim.* 2015;14(3):589–599.

36. Tien CL, Letendre M, Ispas-Szabo P, et al. Development of biodegradable films from whey proteins by cross-linking and entrapment in cellulose. *J Agric Food Chem.* 2000;48(11):5566–5575.

37. Socaciu MI, Fogarasi M, Semeniuc CA, et al. Formulation and characterization of antimicrobial edible films based on whey protein isolate and tarragon essential oil. *Polymers (Basel).* 2020;12(8):1748.

38. Li J, Miao J, Wu J, et al. Preparation and characterization of active gelatin-based films incorporated with natural antioxidants. *Food Hydrocoll.* 2014;37:166–173.

39. Munir S, Hu Y, Liu Y, et al. Enhanced properties of silver carp surimi-based edible films incorporated with pomegranate peel and grape seed extracts under acidic condition. *Food Packag Shelf Life*. 2019;19:114–120.

40. Priyadarshi R, Kim HJ, Rhim JW. Effect of sulfur nanoparticles on properties of alginate-based films for active food packaging applications. *Food Hydrocoll.* 2021;110:106155.

41. Kordali S, Cakir A, Mavi A, et al. Screening of chemical composition and antifungal and antioxidant activities of the essential oils from three Turkish *Artemisia* species. *J Agric Food Chem.* 2005;53(5):1408–1416.

42. Hernández-Muñoz P, Villalobos R, Chiralt A. Effect of cross-linking using aldehydes on properties of glutenin-rich films. *Food Hydrocoll.* 2004;18(3):403-411.

43. Zahedi Y, Fathi-Achachlouei B, Yousefi AR. Physical and mechanical properties of hybrid montmorillonite/zinc oxide reinforced carboxymethyl cellulose nanocomposites. *Int J Biol Macromol.* 2018;108:863–873.

44. Garcia MA, Martino MN, Zaritzky NE. Lipid addition to improve barrier properties of edible starch-based films and coatings. *J Food Sci.* 2000;65(6):941–944.

45. Bourne MC. *Food Texture and Viscosity: Concept and Measurement.* 2nd ed. Elsevier Press; 2003.

46. Gelman A. Analysis of variance. Columbia University Academic Repository. Published 2006. Accessed June 16, 2026.

47. Pallant J. SPSS Survival Manual: A Step by Step Guide to Data Analysis Using IBM SPSS. 6th ed. Routledge; 2020.

48. Krishnaraj C, Jagan EG, Rajasekar S, et al. Synthesis of silver nanoparticles using *Acalypha indica* leaf extracts and its antibacterial activity against water borne pathogens. *Colloids Surf B Biointerfaces.* 2010;76(1):50–56.

49. Ortiz-Zarama MA, Jiménez-Aparicio AR, Lourenço RV, et al. Rheological characterization of solutions of gelatin with bentonite and tannic acid. *Rev Mex Ing Quim.* 2016;15(3):819–830.

50. Araujo-Farro PC, Podadera G, Sobral PJA, et al. Development of films based on quinoa (*Chenopodium quinoa Willdenow*) starch. *Carbohydr Polym.* 2010;81(3):839–848.

51. Nain N, Katoch GK, Kaur S, et al. Recent developments in edible coatings for fresh fruits and vegetables. *J Hortic Res*. 2021;29(2):127–140.

52. Ribeiro AM, Estevinho BN, Rocha F. Preparation and incorporation of functional ingredients in edible films and coatings. *Food Bioprocess Technol.* 2021;14(2):209–231.

53. Li H, Liu C, Sun J, et al. Bioactive edible sodium alginate films incorporated with tannic acid as antimicrobial and antioxidative food packaging. *Foods.* 2022;11(19):3044.

54. Roy S, Rhim JW. Preparation of pectin/agar-based functional films integrated with zinc sulfide nanopetals for active packaging applications. *Colloids Surf B Biointerfaces***.** 2021;207:111999.

55. Podadera G, Sobral PJA, Menegalli FC, et al. Development of films based on quinoa (*Chenopodium quinoa* Willdenow) starch. *Carbohydr Polym.* 2010;81(4):839–848.

56. Praphulla R, Chandraprasad MS, Lakshmi YN, et al. Biosynthesis of silver nanoparticles using lemon extract and its antibacterial activity. *Int J Multidiscip Curr Res*. 2014;2:165–169.

57. Yaman O, Bayındırlı L. Effects of an edible coating and cold storage on shelf-life and quality of cherries. *LWT Food Sci Technol.* 2002;35(2):146–150.

58. Klangmuang P, Sothornvit R. Active coating from hydroxypropyl methylcellulose-based nanocomposite incorporated with Thai essential oils on mango (cv Namdokmai Sithong). *Food Biosci*. 2018;91:541–548.

59. Chen H, Sun Z, Yang H. Effect of carnauba wax-based coating containing glycerol monolaurate on the quality maintenance and shelf life of Indian jujube (Zizyphus mauritiana Lamk.) fruit during storage. *Sci Hortic.* 2019;244:157–164.

60. Khan N, Ullah I, Khan WA, et al. Effect of harvesting stage on quality losses of persimmon fruits during storage. *Madridge J Food Technol.* 2017;2(1):79–84.

61. Naeem A, Abbas T, Ali TM, et al. Effect of guar gum coatings containing essential oils on shelf life and nutritional quality of green-unripe mangoes during low-temperature storage. *Int J Biol Macromol.* 2018;113:403–410.

62. Tanada-Palmu PS, Grosso CRF. Effect of edible wheat gluten-based films and coatings on refrigerated strawberry (*Fragaria* × *ananassa*) quality. *Postharvest Biol Technol*. 2005;36(2):199–208.

63. Hajji S, Younes I, Affes S, et al. Optimization of the formulation of chitosan edible coatings supplemented with carotenoproteins and their use for extending strawberries postharvest life. *Food Hydrocoll.* 2018;83:375–392.

64. Hussain I, Asif M, Ahmed M, et al. Effect of uni-packaging on the postharvest behavior of citrus fruits in NWFP. *Pak J Nutr.* 2004;3(6):336–339.

65. El-Hadidy GA, El-Hadidy EM. Effect of some postharvest treatments on improving quality and storability of persimmon (*Diospyros kaki* L. cv Costata) fruits during cold storage. *Egypt J Agric Res.* 2018;96(4):1357–1472.

66. Gorinstein S, Leontowicz H, Leontowicz M, et al. Influence of two cultivars of persimmon on atherosclerosis indices in rats fed cholesterol-containing diets: investigation *in vitro* and *in vivo*. *Nutrition*. 2011;27(7-8):838–846.

67. Shah HMS, Khan AS, Ali S. Pre-storage kojic acid application delays pericarp browning and maintains antioxidant activities of litchi fruit. *Postharvest Biol Technol.* 2017;132:154–161.

68. Gurjar PS, Killadi B, Lenka J, et al. Effect of gum arabic coatings on physico-chemical and sensory qualities of guava (Psidium guajava L.) cv Shweta. *Int J Curr Microbiol Appl Sci.* 2018;7(5):3769–3775.

69. Abd El-Wahab SM, Kamel HM, Abd El-Hafeez AA, et al. Comparison of different ripening methods for removing astringency in Costata persimmon fruits. *Middle East J Agric Res*. 2017;6(2):569–583.

70. Olivas GI, Barbosa-Cánovas GV. Edible coatings for fresh-cut fruits. *Crit Rev Food Sci Nutr*. 2005;45(7–8):657–670.

71. Shahbazi Y. Application of carboxymethyl cellulose and chitosan coatings containing Mentha spicata essential oil in fresh strawberries. *Int J Biol Macromol.* 2018;112:264–272.

72. Ali S, Khan AS, Malik AU, Shaheen T, et al. Pre-storage methionine treatment inhibits postharvest enzymatic browning of cold-stored Gola litchi fruit. *Postharvest Biol Technol*. 2018;140:100–106.

73. Cedola A, Cardinali A, D'Antuono I, et al. Cereal foods fortified with by-products from the olive oil industry. *Food Biosci.* 2020;33:100490.

74. Dashipour A, Khaksar R, Hosseini H, et al. Antioxidant and antimicrobial carboxymethyl cellulose edible film incorporated with Zataria multiflora essential oil. *Carbohydr Polym.* 2015;72:606–613.

75. Gutiérrez TJ, Alvarez VA, Pérez CJ. Edible films and coatings based on alginate and nanostructured compounds for food preservation. *Food Hydrocoll.* 2018;79:1–14.